The glass transition temperature versus the fictive temperature

Prashanth Badrinarayanan, Wei Zheng, Qingxiu Li, Sindee L. Simon *

Department of Chemical Engineering, Texas Tech University, Lubbock, TX 79409-3121, United States

Abstract

A comparison of the values of the glass transition temperature (T_g) measured on cooling and the limiting fictive temperature (T_f') measured on heating as a function of cooling rate is performed for a polystyrene sample using both capillary dilatometry and differential scanning calorimetry (DSC). The results from both techniques indicate that T_f' is systematically lower than T_g presumably due to the breadth of the relaxation on cooling. The Tool–Narayanaswamy–Moynihan (TNM) model is used to fit the experimental data from dilatometry and DSC in order to ascertain the origins of the higher value of T_g compared to T_f'.
© 2007 Elsevier B.V. All rights reserved.

PACS: 64.70.Pf; 65.60.+a; 81.70.Pg; 82.35.Lr

Keywords: Glass transition; Measurement techniques; Modeling and simulation; Polymers and organics; Calorimetry

1. Introduction

When a glass-forming material is cooled from the equilibrium liquid state, molecular mobility decreases with decreasing temperature; at some point, the time scale for conformational changes becomes comparable to the time scale of cooling and the material deviates from the liquid line and begins to form a glass. The glass transition is, hence, a kinetic rather than a thermodynamic transition and depends on cooling rate [1,2]. The glass transition temperature (T_g), an important characterizing parameter for amorphous materials, is defined as the temperature at which the extrapolated glass and liquid equilibrium lines cross. T_g is correctly measured only on cooling from the equilibrium state [1–3].

A schematic of the specific volume or enthalpy response upon cooling a glass-forming material through T_g to the glassy state is shown in Fig. 1a. Since the glass transition is characterized by a step change in the heat capacity (C_p) or thermal expansivity (α), T_g can also be determined as the point in the transition region where the step change

in heat capacity or thermal expansivity attains half the value of the total step change [3], as shown in Fig. 1b. Dilatometry involves measurement of volume as a function of temperature and T_g is generally evaluated as shown in Fig. 1a. However, calorimetry involves measurement of heat flow or heat capacity as a function of temperature and T_g is evaluated as shown in Fig. 1b.

The fictive temperature (T_f), on the other hand, defines the structure of a glass and can be measured on heating. The fictive temperature is the temperature at which the property of interest, e.g., specific volume or enthalpy, when extrapolated along the glass line intersects the equilibrium liquid line [1,4]. The limiting value of the fictive temperature (T_f') is obtained if the extrapolation is performed from a point deep in the glassy state after cooling at a given rate [4]. T_f' and T_g both depend on the cooling rate, and it is often assumed that the two are equal [4,5]. Plazek and Frund [6] has advocated using T_{fg} as an approximation for T_g at a particular cooling rate, where T_{fg} is the value of T_f obtained using an equal heating rate. Since little relaxation is expected to occur on heating after cooling at the same rate, T_{fg} is essentially equivalent to T_f'. Thus Plazek's [6] method also implies that T_f' measured on heating approximates T_g on cooling.

---

* Corresponding author. Tel.: +1 806 742 1763.
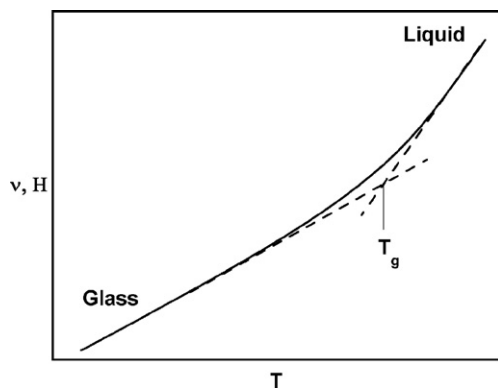 *E-mail address:* sindee.simon@ttu.edu (S.L. Simon).

Fig. 1a. Schematic of the evolution of specific volume (v) or enthalpy (H) with temperature upon cooling from the equilibrium liquid state to the glassy state.
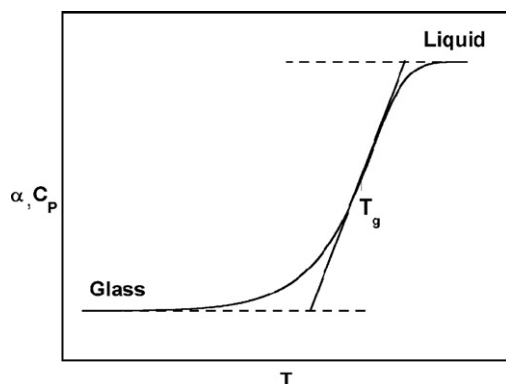

Fig. 2a. Schematic of the specific volume (v) or enthalpy response (H) upon heating at a constant rate m after cooling at rates q_1, q_2, and q_3, respectively, where $q_1 > q_2 > q_3$. T'_{f1}, T'_{f2}, and T'_{f3} represent the corresponding values of limiting fictive temperatures.

Fig. 1b. Schematic of the change in thermal expansivity (α) or the heat capacity (C_p) upon cooling from the equilibrium liquid state to the glassy state.

Fig. 2b. Temperature versus thermal expansivity (α) or heat capacity (C_p) obtained on heating at a rate m after cooling at different rates q_1, q_2, and q_3 such that $q_1 > q_2 > q_3$. T'_{f1}, T'_{f2}, and T'_{f3} represent the corresponding values of limiting fictive temperatures.

A schematic of the specific volume or enthalpy response on heating is shown in Fig. 2a. The glass line overshoots the equilibrium line when the heating rate is higher than the cooling rate due to lower mobility in the glassy state, and the overshoot is accentuated for lower ratios of the cooling and heating rates as shown in the figure. However, if the heating rate is slower than the cooling rate, relaxation will occur along the glass line and lead to an undershoot. The overshoot and undershoot behaviors on heating can also be observed in terms of the response of the heat capacity or thermal expansivity as a function of temperature, as shown in Fig. 2b [7,8]. It is important to recognize that neither the temperature associated with the maximum in the overshoot nor that at half the value of the step change is T'_f. Rather, T'_f must be determined by integration and extrapolation of liquid and glass lines or, equivalently by the following definition given by Moynihan for enthalpy [4]:

$$\int_{T'_f}^{T>T_g} \left(C_{pl} - C_{pg}\right) dT = \int_{T<T_g}^{T>T_g} \left(C_p - C_{pg}\right) dT, \qquad (1)$$

where C_{pg} and C_{pl} refer to the glassy and liquid heat capacities, respectively. An analogous equation can be written for volume replacing C_p with α.
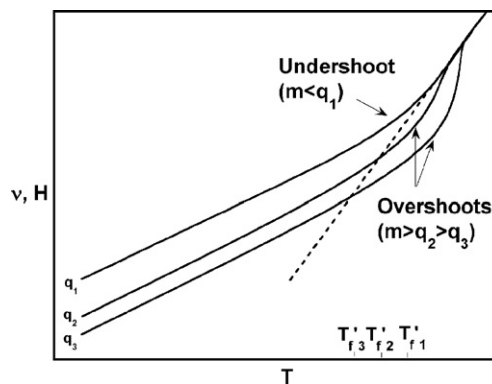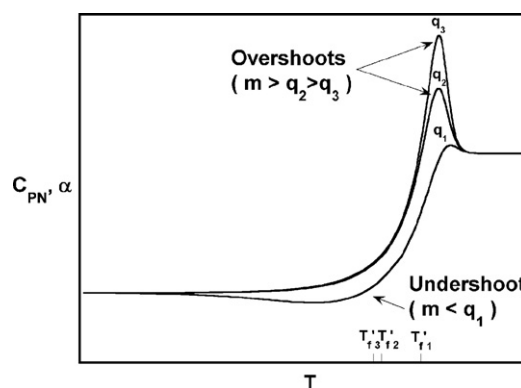
Although T_g can be measured correctly only on cooling, differential scanning calorimetry (DSC) is often used to analyze the glass transition behavior of materials on heating due to historic difficulties controlling the cooling rate and performing the calibration on cooling [1,3,6]; these problems have been resolved with newer instruments and the use of liquid crystal calibration standards that do not supercool [1,9]. However, in spite of the fact that only T'_f can be obtained on heating, the convention of measuring T_g on heating is still used [1,6].

A valid comparison of T'_f and T_g as a function of cooling rate has not previously been made even though several researchers [10–13] have used T'_f to approximate T_g. Plazek and Bero [14] did attempt such a comparison for several glass-forming materials; they performed sequential cooling and heating experiments employing the same rate using differential scanning calorimetry (DSC) and observed that the T'_f obtained on heating was 6 °C higher than T_g measured on cooling. This result is not physically possible as acknowledged in that work [14] and may have been the result of the presence of thermal gradients in the sample

or of inadequate temperature calibrations on cooling. Consequently, a valid comparison of T_g and T_f' as a function of cooling rate is one of the aims of this work.

The experiments in this work were performed with both capillary dilatometry which measures volume changes and DSC which measures heat flow. Using both techniques, the values of T_g on cooling and T_f' on heating are measured as a function of cooling rate. Although, dilatometry has been used successfully to obtain specific volume versus temperature [15–21] and, hence, T_g during cooling, to the best of the authors' knowledge, dilatometry has not been used to obtain the overshoot response and T_f' as a function of the cooling rate. We note that limited dilatometric data showing the overshoot response as a function of aging time has been obtained by Hutchinson and Kovacs [22].

In this work, we also use the Tool–Narayanaswamy–Moynihan (TNM) model [23–25] to fit the experimental data obtained from capillary dilatometry and DSC studies since it is well known that the model captures the nonlinearity and nonexponentiality inherent to the glassy response [8,26]. According to the mathematical treatment of the TNM model [23–25], the relaxation time τ is defined as

$$\tau = \exp\left\{ \ln(A) + \frac{x\Delta h}{RT} + \frac{(1-x)\Delta h}{RT_f} \right\}, \qquad (2)$$

where A is a constant, $\Delta h/R$ represents the relative apparent activation energy, and x is defined in the model as the nonlinearity parameter [8]. Although the temperature dependence for the relaxation time along the equilibrium line follows a WLF [27] or VTHF [28–30] dependence, over a limited temperature range the Arrhenius dependence shown in Eq. (2) is an adequate approximation [8]. The fictive temperature during sequential cooling and heating histories is obtained numerically [25,26] as shown in Eq. (3):

$$T_{f,n} = T_0 + \sum_{i=1}^{n} \Delta T_i \left\{ 1 - \exp\left[-\left(\sum_{j=i}^{n} \frac{\Delta T_j}{q\tau_j} \right)^{\beta} \right] \right\}, \qquad (3)$$

where T_0 is the initial temperature. The temperature histories are incorporated using temperature steps ΔT and the heating or cooling rate q. β is the nonexponentiality parameter. The nonlinearity of the glass transition response is accounted for by the fact that τ_j in Eq. (3) depends on T_f as shown in Eq. (2) [8,24–26,31,32].

Some inadequacies of the TNM model [23–25] have been reported in the literature [8,33–36], including the uncertainty over the physical meaning of the parameters which depend on thermal history [8,33,34], the underestimation of the activation energy parameter [8], and an inability to capture the dependence of the relaxation time on path [35]. Hodge and Huvard [31] and Hutchinson et al. [37] suggested that the discrepancies between the experimental results and the model fits could be due to thermal lag; however, Simon [36] did not observe any improvement in the model performance even after accounting for thermal lag effects. Other attempts to 'fix' the model

have been discussed [8,38,39]. Most recently Hodge [38] has introduced a distribution of activation energies into the model. However, since most of the inadequacies in the model are observed on modeling a broad range of thermal histories and/or deep quenches [8,38] and adequate descriptions of limited DSC and temperature-modulated DSC data have been obtained [8,13,20,25,26,31,32,39–41], in this work we will attempt to use the simplest form of the TNM model [23–25] to describe the cooling and heating dilatometric and DSC histories.

2. Methodology

2.1. Materials

The experiments in this work were performed using a polystyrene (Dylene 8) obtained from Arco polymers. Dylene 8 has a number average molecular weight of 92 800 g/mol and a polydispersity index of 2.38. The same material was also used in previous dilatometric and calorimetric work by Simon and co-workers [20,21,35,40]. Limited aspects of the current work have been published in recent conference proceedings [42,43].

2.2. Dilatometric studies

The capillary dilatometer used in this study was constructed based on Plazek's design following that of Bekkedahl [17,18]. The capillary section comprised of a 5 cm long, 4.68 mm diameter precision bore capillary tube. A detachable stainless steel bulb containing the sample is connected to the other end of the capillary tube using a Kovar glass-to-metal joint. The bulb is sealed tightly using a Viton® o-ring.

Mercury is used as the confining fluid. A Teflon® float is positioned on the meniscus of the mercury in the capillary and is connected to a linear variable differential transformer (LVDT) allowing us to automate measurements [44]. The polystyrene sample used in the capillary dilatometer was molded at 120 °C under vacuum. The diameter of the cylindrical sample obtained was 1.27 cm. In order to minimize thermal gradients and to maximize contact with the confining fluid, a 0.3 cm hole was drilled through the entire length of the sample. The mass of the sample is 5.54 g.

The capillary dilatometer is placed in an oil bath (Model 6025, Hart Scientific) filled with silicone oil. The bath temperatures during the experiments are obtained to an accuracy of 0.0013 K using a platinum resistance thermometer (Black Stack 1560, Hart Scientific). The voltage and temperature data are relayed to a computer through a data acquisition system from National Instruments. An overall resolution of 0.4×10^{-5} cm³/g is obtained by minimizing noise through a low pass filter [21].

The dilatometric cooling experiments were performed from an initial temperature of 105 °C to a final temperature of 60 °C using cooling rates ranging from 0.2 K/min to

0.01 K/min. The initial temperature for the 0.003 K/min cooling experiment was 97.5 °C, still above $T_g(q)$, in order to reduce run time. Note that the sample was at equilibrium density at 97.5 °C before starting this run. After each cooling run, the sample was heated to 105 °C at a rate of 0.2 K/min. To obtain an accurate estimate of the liquid slope, cooling and heating runs were also performed in the temperature range between 120 °C and 105 °C using cooling rates from 0.2 to 0.03 K/min and a heating rate of 0.2 K/min. The average liquid slope was calculated using thirteen runs. (Note that the cooling runs could only be performed from 105 °C rather than from 120 °C to 60 °C due to the limited range of the LVDT.) The absolute specific volumes were obtained by shifting the measured specific volumes to the values obtained at 105 °C in previous work [20] in our laboratory.

The glass transition temperatures (T_gs) were obtained from cooling runs, whereas the limiting fictive temperatures (T_f's) were determined as a function of cooling rate from the heating runs. Since the cooling rate of 0.2 K/min could be maintained only from 105 °C to 85 °C, T_g was obtained for this rate but the limiting fictive temperature was not. The standard deviations in T_g and T_f' were found to be less than 0.2 °C based on repeat runs at several rates. The thermal lags during the cooling and heating runs were calculated [36] based on sample size and geometry. The average value of the thermal lag in the sample was 0.1 °C for cooling or heating at 0.2 K/min. For the other cooling runs, all of which were slower than 0.2 K/min, the average thermal lag was considerably lower; hence, no corrections were made to the experimental data.

2.3. DSC studies

The DSC studies were conducted using a Perkin–Elmer Pyris 1 DSC equipped with an ethylene glycol cooling system maintained at 5 °C. The weights of the sample and reference pans were matched to within 0.02 mg. Aluminum pans were used in all experiments. All runs were performed under a nitrogen atmosphere. For DSC experiments, several samples of masses ranging from 4.02 mg to 10.74 mg were used. The thickness of the samples varied from 0.27 mm to 0.52 mm.

Temperature and heat flow calibrations were performed separately for cooling and heating runs. The temperature calibrations on cooling were performed at the same rates as the sample runs using two liquid crystal standards, (+)-4-*n*-hexylophenyl-4′-(2′-methylbutyl)-biphenyl-4-carboxylate (CE-3 from Leslie [9], University of Alabama; smectic to cholesteric transition at 78.8 °C) and 4,4-azoxy-anisole (Sigma–Aldrich Co. Ltd.; liquid crystal to isotropic liquid transition at 134.5 °C). Indium and both liquid crystal standards were used for temperature calibrations on heating. Heat flow calibrations for cooling and heating were performed using indium.

DSC experiments involved cooling at various rates ranging from 0.01 K/min to 30 K/min, followed by a heating scan at 10 K/min. The starting temperature for the fast cooling runs at 30 K/min and 20 K/min was 170 °C. Other runs were made from 130 °C to 60 °C although runs at the slowest cooling rates were started at lower temperatures with care being taken that the material was in equilibrium prior to starting the run. The glass transition temperatures were determined upon cooling using the half height criteria in the Pyris software. Due to excessive noise at slower cooling rates, the glass transition temperature (T_g) could be determined only for cooling rates equal to or higher than 2 K/min. The limiting fictive temperature (T_f') was determined using the Pyris software from heating scans performed at 10 K/min after each cooling run. Baseline subtraction was performed for all the DSC scans. Two to eight runs were performed on heating; either two or three runs were made for cooling. The standard deviations for T_g and T_f' were found to be within 0.3 °C and 0.2 °C, respectively. The thermal lags between the program temperature and the sample temperature were calculated [36] for all the cooling and heating rates. The average thermal lags upon cooling at 30 K/min for the 0.27 mm and 0.52 mm thick samples were found to be 0.04 °C and 0.14 °C, respectively. The average thermal lag was much lower for slower cooling rates due to the thin geometry of the samples used in the DSC studies; hence, no corrections were made to the experimental data. The effects of instrumental lag were not corrected for.

2.4. Model calculations

For capillary dilatometry, both cooling and heating runs were fit simultaneously with the TNM model [23–25]. Since the 0.2 K/min cooling rate could not be maintained below 85 °C, the data from that cooling run and the heating run which followed were not included for the fit. The specific volumes (v) were calculated from the evolution of T_f with temperature obtained from Eq. (3) using

$$v = v_\infty + v_\infty \Delta\alpha(T_f - T), \tag{4}$$

where v_∞ is the equilibrium specific volume and $\Delta\alpha$ is the difference in thermal expansivity between the liquid and the glassy states. The Levenberg–Marquardt algorithm in Matlab® software was used to optimize the parameters x, β, and $\ln(A)$ for various fixed values of $\Delta h/R$; the final value of $\Delta h/R$ was taken as that corresponding to the minimum value of chi square for the fit [31]. The step sizes in the program were such that the maximum change in T_f was not more than 0.1 °C between steps.

For DSC, the fictive temperatures obtained from model calculations were converted to absolute heat capacity (C_p) as shown below:

$$C_p(T) = C_{pg}(T) + \Delta C_p(T_f)\frac{dT_f}{dT}, \tag{5}$$

where $\Delta C_p(T_f)$ is the difference in heat capacity between the liquid and glassy states evaluated at T_f [4], and dT_f/dT is obtained from Eq. (3). In early attempts to fit DSC data

with the TNM model [23–25], the approximation that $\Delta C_p(T_f)$ equals $\Delta C_p(T)$ was used in order to directly fit the normalized heat capacity $(C_{PN} = (C_p(T) - C_{pg}(T))/\Delta C_p(T))$ [31,32]. However, previous modeling work by Simon [36] suggests that erroneous values of model parameters might be obtained if $\Delta C_p(T_f)$ is assumed to be the same as $\Delta C_p(T)$. Hence, in order to fit the DSC data using the TNM model [23–25], absolute heat capacity measurements were made for Dylene 8 using the step-scan procedure described elsewhere [45]. The absolute liquid and glassy heat capacities are found to depend linearly on temperature:

$$C_{pl}(T) = 0.70 + 0.0031\,T(K)\ \text{J g}^{-1}\ \text{K}^{-1}, \tag{6}$$

$$C_{pg}(T) = 0.02 + 0.0041T(K)\ \text{J g}^{-1}\ \text{K}^{-1}. \tag{7}$$

The value of ΔC_p at temperature T is obtained from the difference of Eqs. (6) and (7). The data obtained on cooling at rates of 30, 10, 4, and 2 K/min and the heating responses which followed were fit simultaneously using a computer program. The data for cooling runs from 1 to 0.01 K/min and the subsequent heating data were not included in the fitting procedure due to the excessive noise in the cooling data at slower rates. The step size in the numerical algorithm was such that the maximum change in T_f was less than 0.2 °C between steps.

3. Results

Specific volume versus temperature curves as a function of cooling rate are shown in Fig. 3. As expected, the specific volume response deviates from the equilibrium line at higher temperatures for higher cooling rates [1–3,6]. The glass transition temperature at each cooling rate is obtained as the point of intersection of the extrapolated liquid line (dashed line) with the extrapolated glass line. T_g decreases from a value of 94.6 ± 0.1 °C at 0.2 K/min to a value of 90.2 °C at 0.003 K/min, as shown in Table
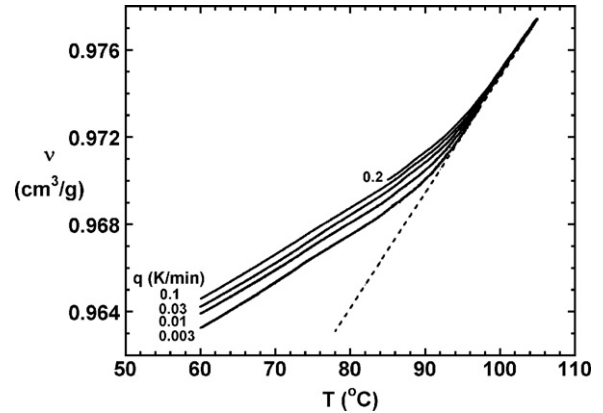

Fig. 3. Specific volume (v) versus temperature (T) curves as a function of the cooling rate (q) from capillary dilatometry. The dashed line represents the equilibrium liquid line.

1. This trend is qualitatively similar to the work of Greiner and co-worker [16] on a different polystyrene sample. The value of T_g at 0.2 K/min is in excellent agreement with previous work in our laboratory on the same material [20,21].

The specific volume response obtained on heating at 0.2 K/min after cooling at various rates is shown in Fig. 4. An overshoot is observed in the curves since the heating rate used in our study is higher than our cooling rates. The overshoot is accentuated as the cooling rate decreases, as expected. To the best of our knowledge, these are the first volume dilatometry curves which capture the overshoot response as a function of the cooling rate. Note that the point of intersection of the heating curves with the equilibrium liquid line does not represent T_f'; rather, the limiting fictive temperature must be obtained by the intersection of the glass line extrapolated from deep in the glassy state with the extrapolated equilibrium liquid line. T_f' is tabulated in Table 1 and is found to decrease with cooling rate, as expected. However, the values of T_f' are

Table 1
Dependence of T_g and T_f' on the cooling rate (q) from capillary dilatometry and DSC

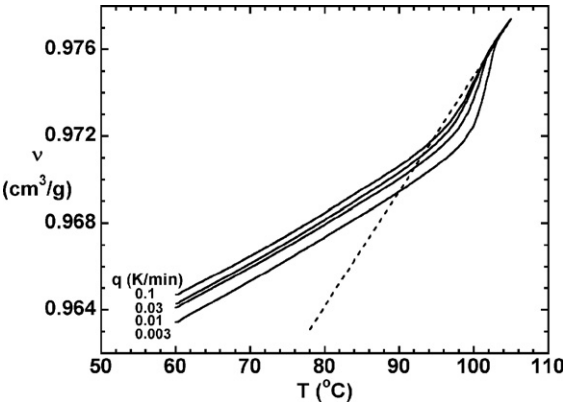|	q (K/min)	T_g (°C)	T_f' (°C)	$T_g - T_f'$ (°C)	$T_g - T_f'$ from model (°C)
Capillary dilatometry	0.2	94.6 ± 0.2	–	–	–
	0.1	93.8	92.4	1.4	0.6
	0.03	92.9 ± 0.2	91.4 ± 0.1	1.5 ± 0.3	0.5
	0.01	91.5	90.6	1.1	0.4
	0.003	90.2	89.5	0.7	0.4
DSC	30	101.5 ± 0.3	100.2 ± 0.1	1.3 ± 0.4	0.9
	20	101.1 ± 0.3	99.7 ± 0.1	1.4 ± 0.4	0.7
	15	100.6 ± 0.1	99.5 ± 0.1	1.1 ± 0.2	0.7
	10	99.9 ± 0.2	99.1 ± 0.2	0.8 ± 0.4	0.5
	4	98.9 ± 0.2	98.4 ± 0.3	0.5 ± 0.5	0.4
	3	–	98.0 ± 0.1	–	–
	2	98.3 ± 0.2	97.5 ± 0.1	0.8 ± 0.3	0.3
	1	–	96.9 ± 0.2	–	–
	0.3	–	95.6 ± 0.1	–	–
	0.1	–	94.5 ± 0.1	–	–
	0.03	–	93.8 ± 0.2	–	–
	0.01	–	92.7 ± 0.2	–	–

Fig. 4. Specific volume (v) versus temperature (T) curves obtained on heating at 0.2 K/min after cooling at the cooling rate (q) specified. The dashed line represents the equilibrium liquid line.

Table 2
Values of apparent $\Delta\alpha$ and ΔC_p for cooling and heating obtained from capillary dilatometer and DSC, respectively

Capillary dilatometer	q (K min^{-1})	$\Delta\alpha$ (10^{-4} K^{-1})	
		Cooling	Heating
	0.1	3.3	3.5
	0.03	3.3 ± 0.1	3.5 ± 0.1
	0.01	3.3	3.5
	0.003	3.3	3.4
DSC	q (K min^{-1})	ΔC_p (J/ g K^{-1})	
		Cooling	Heating
	30	0.221 ± 0.009	0.292 ± 0.004
	20	0.242 ± 0.01	0.294 ± 0.01
	15	0.254 ± 0.002	0.297 ± 0.008
	10	0.251 ± 0.008	0.284 ± 0.008
	4	0.252 ± 0.007	0.291 ± 0.002
	2	0.261 ± 0.009	0.284 ± 0.003

The cooling experiments were performed at the cooling rate (q) specified, while all the heating runs were performed at 0.2 K/min for dilatometry and 10 K/min for DSC.

on average 1.1 °C lower than T_g. The difference between T_g and T'_f arises because the apparent slope of the glass line measured on heating is approximately 10% lower than the value obtained on cooling, as shown in Fig. 5. The values of T_g and T'_f would be equal if a common glass line was used to calculate both values. However, since most measurements of T_g or T'_f are performed using only cooling or only heating runs, respectively, we analyze the cooling and heating runs independently. For such an analysis, it is clear that the apparent glass lines on cooling and heating differ significantly. The difference in the apparent glass slopes (α_g) on heating and cooling leads to a difference in the apparent values of $\Delta\alpha$ (the difference in thermal expansivity between the liquid and glassy state) obtained on heating and cooling. The apparent values of $\Delta\alpha$ for the cooling and heating experiments are shown in Table 2; $\Delta\alpha$ is on average 6% greater on heating. It is emphasized that these differences arise from the breadth of the relaxation through T_g on cooling. If absolute measurements were performed deep enough in the glassy state, the glass lines on heating
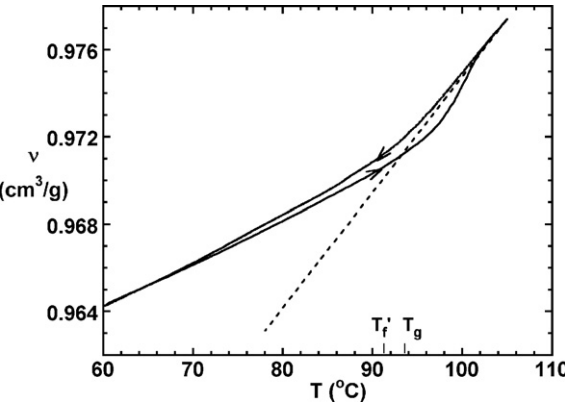
and cooling will be the same. However, cooling to 40 °C below T_g is not adequate to obtain the correct value of α_g on cooling for this material.

In order to compare the volumetric and enthalpic responses, similar cooling and heating experiments were also performed using DSC. The normalized heat capacity (C_{PN}) versus temperature curves obtained on cooling are shown in Fig. 6. As expected, and in agreement with dilatometric results, T_g decreases with decreasing cooling rate. T_g decreases from a value of 101.5 ± 0.3 °C at 30 K/min to 98.3 ± 0.2 °C at 2 K/min, as shown in Table 1. The DSC enthalpic response on heating at 10 K/min after cooling at various rates is shown in Fig. 7. As expected and again consistent with dilatometric results, the overshoot increases and T'_f decreases with decreasing cooling rates. Similarly, T'_f measured on heating is on average 0.9 °C lower than T_g measured on cooling. Also in analogy to the dilatometry results, the apparent difference in the heat capacity between
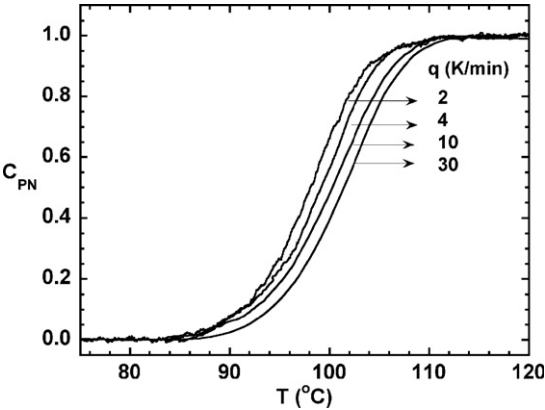

Fig. 5. Determination of T_g and T'_f for cooling at 0.03 K/min followed by heating at 0.2 K/min. T_g and T'_f are indicated and were obtained from the point of intersection of the equilibrium line (dashed line) with the glass lines obtained independently form the cooling and heating curves, respectively.

Fig. 6. Normalized heat capacity (C_{PN}) as a function of the cooling rate (q) obtained from DSC.
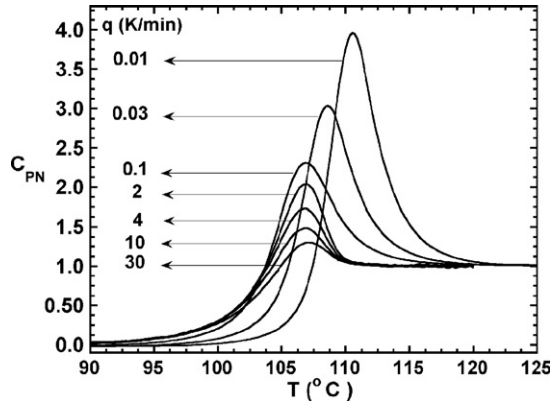
Fig. 7. Normalized heat capacity (C_{PN}) versus temperature (T) on heating at 10 K/min as a function of the cooling rate (q).
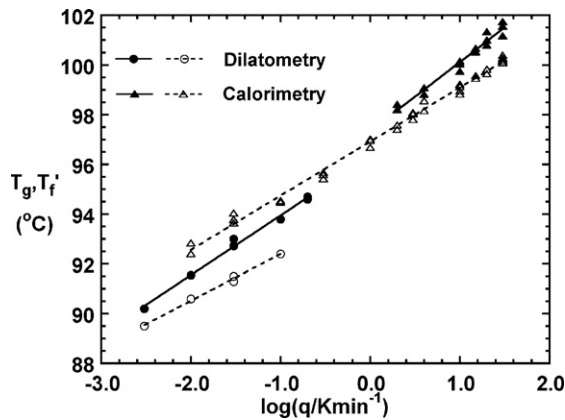

Fig. 8. Dependence of T_g and T'_f on the cooling rate (q) for dilatometry and DSC. The solid symbols represent the T_g values and the open symbols represent T'_f values. The solid lines and the dashed lines represent the best fits to T_g and T'_f data, respectively.

the liquid and the glassy states (ΔC_p) is found to be on average 17% larger on heating than on cooling; values of the apparent ΔC_p are tabulated in Table 2. Again, we emphasize that ΔC_p should be the same on cooling and heating if absolute measurements are made to deep enough in the glassy state and tangents are taken using the correct glass line. However, typical DSC measurements do not report absolute C_p and problems with the baseline do not allow ΔC_p to be determined using tangents far from the transition. Consequently, our result typifies problems with measuring ΔC_p using DSC.

The values of T_g and T'_f as a function of cooling rate for both capillary dilatometry and DSC studies are com-

pared in Fig. 8. In both dilatometry and DSC, the values of T'_f are on average approximately 1 °C lower than T_g at rates where both are measured. Upon extrapolating to the same cooling rates, the calorimetric values of T_g and T'_f are higher than the dilatometric values by 1 °C and 2 °C, respectively. Since different measurement techniques might capture different relaxation distributions in a material, differences in T_g between various measurement techniques are not necessarily unexpected, as pointed out by Moynihan [5]. Furthermore, in this work the glassy behavior was not determined using the same temperature range in dilatometry and DSC, and this might lead to different values of T_g at the same cooling rate.

The best fit values of the slopes $dT_g/d\log q$ and $dT'_f/d\log q$ for both dilatometry and DSC are compared in Table 3 along with literature values [16,20,31,39,40,46–52], with the errors representing the standard errors of the fits. The values of $dT_g/d\log q$ in this work are comparable with the dilatometric results reported by Greiner and Schwarzl [16]($dT_g/d\log q = 2.9$), and the values of $dT'_f/d\log q$ are in agreement with the value obtained by analyzing the calorimetric data of Dueñas and co-workers [46] for a polystyrene of similar molecular weight ($dT'_f/d\log q = 2.2 \pm 0.1$). Other values in the literature range from 2.3 to 4.1 K [20,31,39,40,47–52], as shown in Table 4. Based on a t-test at 90% confidence interval, the values of $dT_g/d\log q$ from capillary dilatometry and DSC in this work are found to be statistically similar. Furthermore, the values of $dT'_f/d\log q$ from capillary dilatometry and DSC are also found to be statistically similar. However, for dilatometry and DSC, the values of $dT_g/d\log q$ are found to be at least 5% and 16% greater than the values of $dT'_f/d\log q$, respectively.

Table 4
TNM model parameters for capillary dilatometry and DSC

Parameter	Capillary dilatometry	DSC
$\Delta h/R$ (kK)	130.1 ± 0.8	82.7 ± 0.9
$\ln(A/s)$	-344.70 ± 0.02	-217.05 ± 0.02
x	0.258 ± 0.002	0.426 ± 0.006
β	0.451 ± 0.005	0.602 ± 0.005

The best fit parameters are obtained simultaneously fitting cooling and heating runs as described in the text. Since $\Delta h/R$ and $\ln(A)$ were strongly correlated, varying $\Delta h/R$ without varying $\ln(A)$ resulted in large changes in chi square. Hence, the error in $\Delta h/R$ was determined by varying $\Delta h/R$ while maintaining x, β, and $\ln(\tau_{Tg})$ constant.

Table 3
Comparison of the cooling rate dependence of T_g and T'_f from capillary dilatometry and DSC

Source	$dT_g/d\log q$ (K)	$dT'_f/d\log q$ (K)	$dT_g/d\log q$ or $dT'_f/d\log q$ (K)
Capillary dilatometry	2.4 ± 0.1	1.9 ± 0.1	
DSC	2.8 ± 0.1	2.2 ± 0.03	
Literature [16,20,31,39,40,46–52][a]			2.3–4.1

[a] Most of the individual values included here are also listed elsewhere [40].

4. Discussion

The values of the limiting fictive temperature obtained on heating as a function of cooling rate are found to be between 0.2 and 1.5 °C lower than the values of T_g for dilatometry and DSC, presumably due to the breadth of the relaxation through T_g on cooling. The case for the broad relaxation on cooling is further corroborated by the lower apparent glass slopes (α_g and C_{pg}) and the higher apparent values of $\Delta\alpha$ and ΔC_p obtained on heating. This supposition is tested by comparing the predictions from TNM model [23–25] calculations with experimental results. The TNM model [23–25] calculations for the specific volume response on cooling at various rates are compared with experimental data in Fig. 9. The model provides a good description of the specific volume response on cooling at various rates although slight deviations are observed at a cooling rate of 0.003 K/min. The TNM model [23–25] calculations for the specific volume response observed on heating at 0.2 K/min after various cooling histories are shown in Fig. 10 (using the same model parameters as for the fit shown in Fig. 9). The model again provides an excellent description of the overshoot response although slight deviations are observed in the glassy regions. The model parameters obtained by simultaneously fitting both cooling and heating data are tabulated in Table 4. The value of the activation parameter ($\Delta h/R$) from model calculations is found to be in excellent agreement with the value determined experimentally ($\Delta h/R = 127 \pm 5$ kK) from the cooling rate dependence of T_g. The error of each fitting parameter was determined by calculating chi square of the fit as a function of the parameter of interest holding the other parameters constant; the error for each parameter shown in Table 4 represents the change which results in a chi square 1% greater than the minimum value. Furthermore, the errors were also calculated from the covariance matrix for the optimized fit parameters, since the diagonal elements of the covariance matrix represent the square of
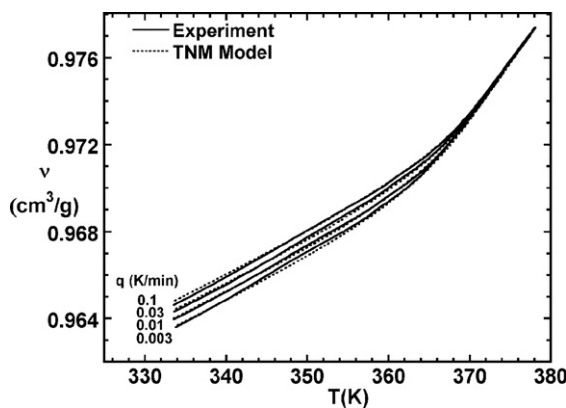

Fig. 10. Comparison of overshoot response observed on heating as a function of cooling rate (q) from TNM model calculations (dashed lines) and capillary dilatometry (solid lines). The values of the best fit parameters are $\Delta h/R = 130.1$ kK, $x = 0.258$, $\beta = 0.451$, and $\ln(A/s) = -344.70$.
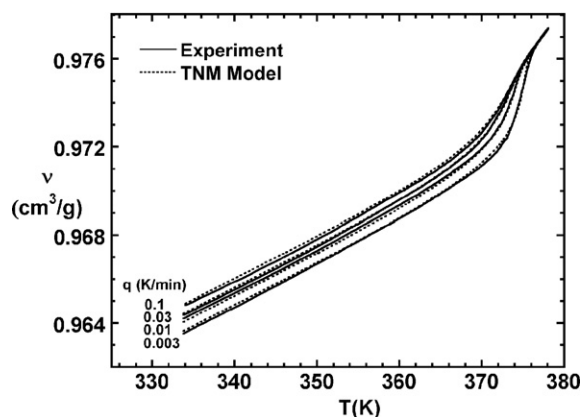
the standard error of the fit parameters [53,54]. The values of the errors determined from this method were at least two times smaller compared to the errors reported in Table 4.

The TNM model [23–25] calculations for the volumetric data are used for a comparison of values of T_g and T'_f, as shown in Fig. 11. The TNM model calculations for cooling at 0.003 K/min followed by heating at 0.2 K/min, shown as the dashed lines in the figure, have been shifted vertically to facilitate a comparison with the experimental data (solid lines). For the experimental data, the apparent glass line on heating exhibits a lower slope than the glass line on cooling; hence, the value of T_g is greater than the value of T'_f by 0.7 K. The model calculations for the same thermal history also show a lower glass slope on heating and predict that the value of T_g is 0.4 K higher than the corresponding value of T'_f if the cooling and heating runs are analyzed independently; however, as previously emphasized, the two values are equal if the same glass line is used for determination of T_g and T'_f. The differences between T_g

Fig. 9. Comparison of specific volume response on cooling as a function of cooling rate (q) from TNM model calculations (dashed lines) and capillary dilatometry (solid lines). The values of the best fit parameters are $\Delta h/R = 130.1$ kK, $x = 0.258$, $\beta = 0.451$, and $\ln(A/s) = -344.70$.
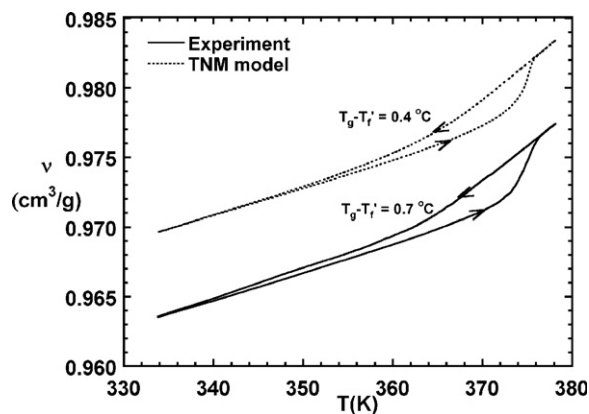

Fig. 11. Comparison of specific volume response obtained from TNM model calculations (dashed lines) and capillary dilatometry (solid lines) for cooling at 0.003 K/min followed by heating at 0.2 K/min. The values of the model parameters are $\Delta h/R = 130.1$ kK, $x = 0.258$, $\beta = 0.451$, and $\ln(A/s) = -344.70$.

and T_f' from model calculations (obtained by analyzing the cooling and heating runs independently) are compared with experimental results as function of cooling rate in Table 1.

For DSC studies, significantly different values of the nonlinearity parameter x are required to obtain suitable fits of the heat capacity responses on cooling and on heating, respectively, and the model is unable to provide an adequate description of the cooling data, as shown in Fig. 12. However, the model provides an adequate description of the heat capacity response observed on heating, although some small disagreement is observed when heating at 10 K/min follows cooling at 30 K/min, as shown in Fig. 13 in the temperature region just preceding the overshoot. We also note that the differences between the experimental and model data on cooling may result in part from errors in the experimental curves due to use of an improper glass line due to the reasons previously cited (the fact that absolute C_p is not measured and baseline curvature). The
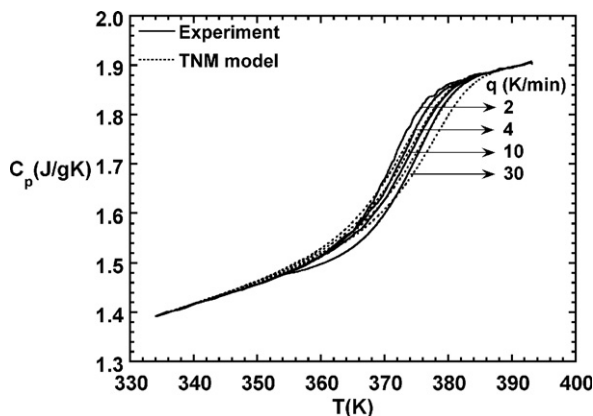

Fig. 12. Comparison of heat capacity response as a function of cooling rate (q) from TNM model calculations (dashed lines) and transformed DSC data (solid lines). The values of the model parameters are $\Delta h/R = 82.7$ kK, $x = 0.426$, $\beta = 0.602$, and $\ln(A/s) = -217.05$.

Fig. 13. Comparison of heat capacity response obtained on heating at 10 K/min as a function of cooling rate (q) from TNM model calculations (dashed lines) and transformed DSC data (solid lines). The values of the model parameters are $\Delta h/R = 82.7$ kK, $x = 0.426$, $\beta = 0.602$, and $\ln(A/s) = -217.05$.
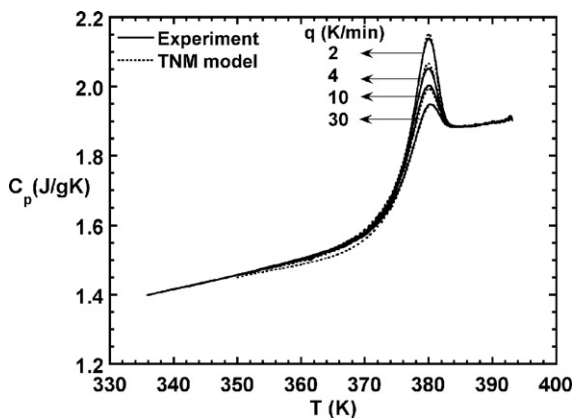
values of TNM model [23–25] parameters obtained from simultaneously fitting DSC data obtained on cooling and heating are shown in Table 4. The parameters are found to be in good agreement with the average values of parameters for polystyrene reported by Hodge [8,31]. The value of the activation parameter ($\Delta h/R$) from model calculations for the calorimetric data is found to be lower than the value determined experimentally from the cooling rate dependence of T_g (82.7 ± 0.9 kK versus 144 ± 2 kK), also in agreement with literature [8]. The values of the difference between T_g and T_f' from model calculations are compared with experimental values in Table 1. The model reproduces the experimental result of $T_g > T_f'$ in spite of the fact that the absolute values of T_g and T_f' from the model calculations differ from the experimental values since a smaller value of $\Delta h/R$ is needed in the model to correctly describe the enthalpy overshoot.

Both experiments and model calculations for capillary dilatometry and DSC predict a difference between T_g and T_f', although the difference is smaller for the model calculations. This indicates that cooling to only 60 °C (40 °C below T_g) does not facilitate an accurate estimation of the glass slope on cooling. When the final temperature of the cooling runs is changed to 40 °C in the model calculations, the difference between T_g and T_f' decreases significantly; for example, the difference between the dilatometric T_g and T_f' for a cooling rate of 0.003 K/min is calculated to decrease from 0.4 K to 0.1 K. Similarly, the difference between the calorimetric T_g and T_f' for a cooling rate of 2 K/min is calculated to decrease from 0.3 K to 0.1 K. The decrease in the difference between T_g and T_f' upon quenching deeper in to the glassy state validates our supposition that the difference is an artifact of the breadth of the relaxation on cooling. Experimentally, however, since absolute measurements are not generally made to deep in the glass state, especially for calorimetry, it is important for researchers to be aware of the differences between T_g and T_f' and to be aware of the limitations of their measurements.

5. Conclusions

In this work the values of T_g and T_f' of a polystyrene are reported as a function of cooling rate using capillary dilatometry and DSC. T_g is obtained from cooling, whereas T_f' is obtained from heating. For both dilatometric and DSC studies, T_f' is found to be approximately 1 °C lower than T_g due to the fact that the apparent glass slopes (α_g and C_{pg}) obtained on heating are smaller than the values obtained on cooling, or alternatively, that the apparent values of $\Delta\alpha$ and ΔC_p obtained on heating are greater than the values obtained on cooling. These differences are attributed to the breadth of the relaxation through T_g on cooling. If the same glassy line is used to evaluate cooling and heating curves, the values of T_g and T_f' would be equal; however, cooling to even 40 °C below T_g is not deep enough in the glass to yield the correct glass line for the polystyrene

studied. The values of $dT_g/d\log q$ and $dT'_f/d\log q$ from capillary dilatometry were found to be in agreement with corresponding values from DSC studies based on a *t*-test at 90% confidence. However, for dilatometry and DSC, the values of $dT_g/d\log q$ were at least 5% and 16% greater than $dT'_f/d\log q$, respectively.

TNM model [23–25] calculations are found to provide an adequate description of the cooling response and the overshoot response on heating using a single set of parameters for capillary dilatometry. The model provided an adequate description of the overshoot response on heating for DSC studies; however, the same parameter set could not capture the heat capacity response on cooling. TNM model [23–25] calculations for capillary dilatometry and DSC clearly indicate a higher value of T_g compared to T'_f for thermal histories examined in this work when the cooling and heating curves are analyzed independently, in agreement with experimental results. We suggest that the difference is brought about by the breadth of the relaxation on cooling, which is confirmed by TNM model [23–25] calculations.

Acknowledgments

References

[1] D.J. Plazek, K.L. Ngai, in: J.E. Mark (Ed.), Physical Properties of Polymers Handbook, American Institute of Physics, Woodbury, NY, 1996.

[2] G.B. McKenna, in: C. Booth, C. Price (Eds.), Comprehensive Polymer Science, Polymer Properties, Vol. 2, Pergamon, Oxford, 1989 (Chapter 2).

[3] G.B. McKenna, S.L. Simon, in: S.Z.D. Cheng (Ed.), Handbook of Thermal Analysis and Calorimetry, Applications to Polymers and Plastics, Vol. 3, Elsevier Science, 2002.

[4] C.T. Moynihan, A.J. Easteal, M.A. DeBolt, J. Tucker, J. Am. Ceram. Soc. 59 (1976) 12.

[5] C.T. Moynihan, in: R.J. Seyler (Ed.), Assignment of the Glass Transition, ASTM, Philadelphia, PA, 1994.

[6] D.J. Plazek, Z.N. Frund Jr., J. Polym. Sci. B: Pol. Phys. 28 (4) (1990) 431.

[7] B. Wunderlich, in: R.J. Seyler (Ed.), Assignment of the Glass Transition, ASTM, Philadelphia, PA, 1994.

[8] I.M. Hodge, J. Non-Cryst. Solids 169 (3) (1994) 211.

[9] J.D. Menczel, T.M. Leslie, Thermochim. Acta 166 (1990) 309.

[10] J.-Y. Park, G.B. McKenna, Phys. Rev. B 61 (10) (2000) 6667.

[11] P. Bernazzani, S.L. Simon, D.J. Plazek, K.L. Ngai, Eur. Phys. J. E8 (2) (2002) 201.

[12] S.L. Simon, P. Bernazzani, G.B. McKenna, Polymer 44 (26) (2003) 8025.

[13] S. Montserrat, Y. Calventus, J.M. Hutchinson, Polymer 46 (26) (2005) 12181.

[14] D.J. Plazek, C.A. Bero, J. Phys. Condens. Mat. 15 (11) (2003) S789.

[15] A.J. Kovacs, Fortschritte der Hochpolymeren-Forschung 3 (1963) 394.

[16] R. Greiner, F.R. Schwarzl, Rheol. Acta 23 (1984) 378.

[17] C.A. Bero, D.J. Plazek, J. Polym. Sci. B: Pol. Phys. 29 (1) (1991) 39.

[18] N. Bekkedahl, J. Res. Nat. Bur. Stand. 42 (1949) 145.

[19] C.A. Bero, PhD thesis, University of Pittsburg, 1994.

[20] S.L. Simon, J.W. Sobieski, D.J. Plazek, Polymer 42 (6) (2001) 2555.

[21] P. Bernazzani, S.L. Simon, J. Non-Cryst. Solids 307 (2002) 470.

[22] J.M. Hutchinson, A.J. Kovacs, J. Polym. Sci. B: Pol. Phys. 4 (1976) 1575.

[23] A.Q. Tool, J. Am. Ceram. Soc. 29 (1946) 240.

[24] O.S. Narayanaswamy, J. Am. Ceram. Soc. 54 (1971) 491.

[25] C.T. Moynihan, P.B. Macedo, C.J. Montrose, P.K. Gupta, M.A. DeBolt, J.F. Dill, B.E. Dom, P.W. Drake, A.J. Easteal, P.B. Elterman, R.P. Moeller, H. Sasabe, J.A. Wilder, Ann. NY. Acad. Sci. 279 (1976) 15.

[26] I.M. Hodge, A.R. Berens, Macromolecules 15 (3) (1982) 762.

[27] M.L. Williams, R.F. Landell, J.D. Ferry, J. Am. Chem. Soc. 77 (1955) 3701.

[28] H. Vogel, Phys. Z. 22 (1921) 645.

[29] G. Tammann, G. Hesse, Z. Anorg. Allg. Chem. 156 (1926) 245.

[30] G.S. Fulcher, J. Am. Chem. Soc. 8 (1925) 339.

[31] I.M. Hodge, G.S. Huvard, Macromolecules 16 (3) (1983) 371.

[32] I.M. Hodge, Macromolecules 16 (6) (1983) 898.

[33] I.M. Hodge, Macromolecules 19 (3) (1986) 936.

[34] I.M. Hodge, Macromolecules 20 (11) (1987) 2897.

[35] S.L. Simon, P. Bernazzani, J. Non-Cryst. Solids 352 (2006) 4763.

[36] S.L. Simon, Macromolecules 30 (14) (1997) 4056.

[37] J.M. Hutchinson, M. Ruddy, M.R. Wilson, Polymer 29 (1) (1988) 152.

[38] I.M. Hodge, J. Chem. Phys. 123 (12) (2005) 124503.

[39] S. Weyer, M. Merzylokov, C. Schick, Thermochim. Acta 377 (1&2) (2001) 85.

[40] Q. Li, S.L. Simon, Polymer 47 (13) (2006) 4781.

[41] S. Weyer, H. Huth, C. Schick, Polymer 46 (26) (2005) 12240.

[42] P. Badrinarayanan, W. Zheng, S.L. Simon, in: Proceedings: Annual Technical Conference (ANTEC), Society of Plastics Engineers, 2006, p. 1669.

[43] P. Badrinarayanan, S.L. Simon, in: Proceedings of the 34th NATAS Conference, 2006, p.142.

[44] R.S. Duran, G.B. McKenna, J. Rheol. 34 (1990) 813.

[45] D. Huang, S.L. Simon, G.B. McKenna, J. Chem. Phys. 122 (8) (2005) 084907.

[46] F.H. Sanchez, J.M.M. Dueñas, J.L.G. Ribelles, J. Therm. Anal. Calorim. 72 (2) (2003) 631.

[47] J.M. O' Reilly, I.M. Hodge, J. Non-Cryst. Solids 131 (1991) 451.

[48] G.C. Stevens, M.J. Richardson, Polym. Commun. 26 (1985) 77.

[49] W.M. Prest Jr., F.J. Roberts, I.M. Hodge, in: Proceedings of the 12th NATAS Conference, 1983, p. 119.

[50] L. Aras, M.J. Richardson, Polymer 30 (12) (1989) 2246.

[51] V.P. Privalko, S.S. Demchenko, Y.S. Lipatov, Macromolecules 19 (3) (1986) 901.

[52] B. Wunderlich, D.M. Bodily, M.H. Kaplan, J. Appl. Phys. 35 (1964) 95.

[53] W.H. Press, B.P. Flannery, S.A. Teukolsky, W.T. Vetterling, Numerical Recipes in C++: The Art of Scientific Computing, Cambridge University, Cambridge, 2002.

[54] Y. Bard, Nonlinear Parameter Estimation, Academic, NY, 1974.